Hindawi
Advances in Civil Engineering
Volume 2018, Article ID 9130835, 10 pages
https://doi.org/10.1155/2018/9130835

Research Article

Consolidated Undrained Triaxial Compression Tests and Strength Criterion of Solidified Dredged Materials

Jianwen Ding[1], **Xusong Feng**[2], **Yupeng Cao**[3], **Sen Qian**[4] and **Feng Ji**[5]

[1]*Ph.D, Associate Professor, Institute of Geotechnical Engineering, School of Transportation, Southeast University, Nanjing 210096, China*
[2]*Ph.D, Jiangsu Water Resources Company Limited, The Water Diversion Project from South to North in China, Nanjing 210029, China*
[3]*Ph.D, Lecturer, College of Transportation, Shandong University of Science and Technology, Qingdao 266590, China*
[4]*Ph.D Candidate, Institute of Geotechnical Engineering, School of Transportation, Southeast University, Nanjing 210096, China*
[5]*Ph.D, Jiangsu Water Resources Company Limited, The Water Diversion Project from South to North in China, Nanjing 210029, China*

Correspondence should be addressed to Jianwen Ding; jwding2006@163.com

Received 14 May 2018; Accepted 18 August 2018; Published 15 October 2018

Academic Editor: Yonggui Chen

Consolidated undrained triaxial compression tests were performed to investigate the shear strength behavior of the solidified dredged materials (SDM). The variation law of deviator stress and excess pore water pressure with the increase of the applied confining pressure was investigated. It is found that the shear strength envelope is consisted of two lines, and there exists a transitional stress on the intersection point. The undrained shear strength develops slightly with the increase of applied normal stress in the preyield state. However, the undrained shear strength increases significantly in the postyield state, and the strength envelope is nearly a straight line with the extension through the origin. Based on the triaxial test data and the binary medium model, a strength criterion considering strength evolution mechanism is proposed and the relevant parameters of the strength criterion were discussed. Comparisons of the predicted results and experimental data demonstrate that the proposed strength criterion can properly describe the strength evolution rules of the SDM.

1. Introduction

Large volumes of sediment are dredged annually to maintain the navigational depth of channels and harbors, to prevent rivers from flooding, and to restore the ecosystem of degenerative water bodies [1–6]. How to deal with the vast amounts of dredged materials (DM) becomes an important issue in engineering practice. Many studies have been conducted regarding the use of DM as land reclamations backfill or engineering construction materials [2, 5, 7–9]. Solidification/stabilization is an ideal way that can improve the engineering properties of the abandoned DM [5] (Kamon et al. 2005) [6, 8, 10], showing economical and environmental advantages and avoiding borrowing soils from elsewhere.

The strength properties of structured clays are different from remolded clays [11–15]. However, the existing strength criterions are mostly established on the basis of the properties of reconstituted soils [16–19] that cannot well reflect the influence of soil structures on the properties of structured soils [14]. It has been well reported by researchers [15, 20] that the strength envelope of the natural structured sedimentary clays can be divided into two parts in terms of the structure yield stress (i.e., preyield state and postyield state). And there also exists a transitional stress on the strength envelope of the cement-treated soil [21, 22]. The structure formation of natural soil is attributed to the soil structure development during depositional and post-depositional processes [23–26]. Similar to natural structured soils, the observed high yield stresses are evidences for the

structure of cement-treated soil [1, 2, 22, 27, 28]. The structure of the SDM is formed by cement hydration and pozzolanic reaction, and a mechanically stable soil matrix was produced due to cementation bonds [1, 6, 21, 28, 29]. Hence, the SDM can be considered as an artificially structured soil, and it can exhibit strongly stable structure and higher yield stress compared with the untreated DM.

The objectives of this study are (1) to investigate shear strength behavior of the SDM, (2) to establish strength criterion for the SDM, and (3) to verify the validity of the proposed strength criterion and discuss the relevant parameters.

2. Materials and Test Method

2.1. Materials. The dredged material (DM, as shown in Figure 1) used in this study was taken from the bottom of the Baima Lake located in Huaian, Jiangsu Province, China (sampling site as shown in Figure 2). The basic physical properties of the DM are summarized in Table 1. The liquid limit and plastic limit are 66.1% and 26.6%, respectively. According to the Unified Soil Classification System, the DM is classified as high plasticity clay.

Based on the conventional cement-treated method, in this study, phosphogypsum was used together with cement to stabilize the DM at high water content. It should be mentioned that phosphogypsum is a by-product of the production of phosphoric acid, only a small portion can be recycled, other most is deposited without any prior treatment. Deserted phosphogypsum occupies land areas and possibly causes serious environmental contamination [31–33]. Type I ordinary Portland cement was used in this study, and phosphogypsum (as shown in Figure 3) used here was taken from a chemical company in Nanjing, China.

2.2. Sample Preparing and Test Method. Mixing proportion design of the SDM is presented in Table 2, and current dredging method characterized with high water content of the DM [34] has been taken into account. In Table 2, the mixing proportion can be expressed as 2.5W+C100+P40 and so on. In the expression, 2.5W denotes the water content of DM slurry is 2.5 times the liquid limit, C100 denotes the cement content is 100 kg for 1 m^3 DM slurry (i.e., 100 kg/m^3), and P40 denotes the weight of phosphogypsum is 40% of the cement. All triaxial tests were performed at the curing period of 28 days, and the confining pressure is designed in the range of 100–1200 kPa, which are shown in Table 2.

The specimens were prepared by mixing the DM slurries with dry cement powder and phosphogypsum powder. Then, the uniform paste was placed into a cylindrical mold. The bottom of the mold is specially designed which can be dismantled freely so that the sample is easy to dismantle. Friction was minimized by using a polished inner wall and smeared with a thin film of grease. The cylindrical specimens were dismantled after 24 hours, wrapped with plastic bags, and then stored in a standard curing room with a constant ambient temperature of $20 \pm 2^{\circ}C$ and a relative humidity above 95%. The dimension of all specimens (as shown in Figure 4) is 39.1 mm in diameter and 80 mm in height.

Consolidated undrained triaxial compression tests were conducted at the designed curing period of 28 days. Before installation in the triaxial cell, the specimens were placed in a vacuum chamber filled with distilled water for saturation at least 24 hours. After installation, undrained isotropic loading was used to check the pore pressure coefficient "B." The triaxial tests were conducted at an axial compression rate of 0.073 mm/min. Excess pore water pressure was measured during the shear phase. It should be mentioned that even adopted with a back pressure of 200 kPa after vacuum saturation, the measured pore pressure parameter "B" was only around 0.9, which is in agreement with the phenomenon reported by Kamruzzaman et al. [28].

3. Results and Discussion

The variation of deviator stress under different confining pressures is shown in Figure 5. It can be seen that there exists a peak deviator stress for all SDM samples, which is similar to the overconsolidated soils [28, 35–39]. Figure 5 illustrates that the peak deviator stress increases with the applied confining pressure and the failure strain also increases with the increase in confining pressure. It is interesting to note that the increment of the peak deviator stress is different under different stress levels. The peak deviator stress increases very small when the confining pressure is less than 400 kPa, which is similar to the observations reported by other researchers [21, 28]. The change of the fabric in the consolidation process is insignificant at low confining pressures, and the peak strength is mainly governed by the soil structure resistance [15, 21]. However, the peak strength significantly increases when the confining pressure is more than 400 kPa, for the cementation bond begins to break and its artificial structure disappears progressively at high confining pressures, and the shear strength mainly depends on the applied stress level. Hence, the behavior of the SDM is similar to heavily over-consolidated natural structured clays, although its structure yield stress is related to bonding and not to stress history [1, 22, 28, 40].

The variation of excess pore water pressure under different confining stress is shown in Figure 6. It can be seen that there exists a peak value when the confining pressure is lower than 400 kPa; however, the peak value becomes insignificant when the confining pressure is greater than 400 kPa. Similar results were observed by other researchers on cement-treated or untreated clays [28, 41, 42]. The change law of excess pore water pressure with the confining pressure is different with the deviator stress, the peak pore water pressure increases notably with an increase in confining pressure, both in the lower stress level stage and in the higher stress level stage. Similar results were reported by other researchers on cement-treated clays [28, 41].

The relationship between undrained shear strength and applied normal stress is shown in Figure 7. It can be seen that the undrained shear strength envelope is approximately consisted of two straight lines, and there is a transitional

Figure 1: Dredged material.

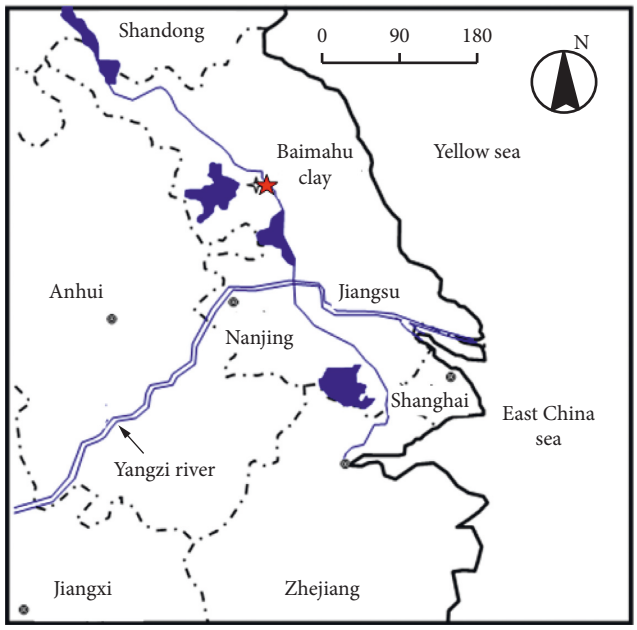

Figure 2: Sampling site [30].

Table 1: Basic physical properties of the dredged material.

Properties	Values
Specific gravity, G_s	2.68
Liquid limit, LL (%)	66.1
Plastic limit, PL (%)	26.6
Plasticity index, PI (%)	39.5
Sand (>0.074 mm) content (%)	9.0
Silt (0.074–0.005 mm) content (%)	59.4
Clay (<0.005 mm) content (%)	31.6
Organic content (%)	2.2

Figure 3: Phosphogypsum.

Table 2: Programme of triaxial test.

Mixing proportion	Confining pressure (kPa)
2.5W+C100+P40	100, 200, 400, 600, 800, 1000, 1200
3.0W+C100+P70	100, 200, 400, 600, 800, 1000, 1200
3.0W+C200	100, 200, 400, 600, 800, 1000, 1200
3.0W+C200+P50	100, 200, 400, 600, 800, 1000, 1200

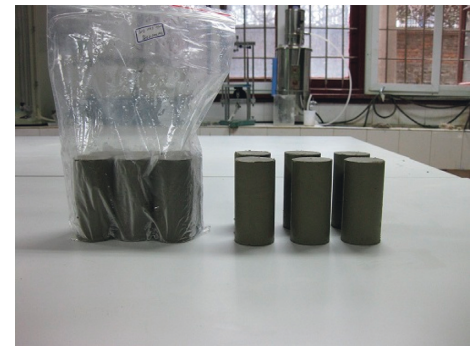

Figure 4: Specimens.

stress at the intersection point of the two straight lines on the strength envelope. Such a bilinear strength envelope for natural sedimentary clays has been well reported by other researchers [15, 20].

In Figure 7, it can be seen that the undrained shear strength increases slightly with the increase in applied normal stress at first (i.e., in the preyield state), which indicates that the shear strength of the SDM is mainly affected by the soil structure resistance when the applied stress is smaller than the yield stress. However, the shear strength increases significantly when the applied normal stress is greater than yield stress (i.e., in the postyield state). It is interesting to note that all the strength envelopes are nearly a straight line with the extension through the origin, which is consistent with the observation of other researchers [15, 22]. It indicates that the undrained shear strength mainly depends on the applied normal stress in the postyield stage, for the cementation bond is progressively destroyed and the soil structure resistance gradually vanishes when the stress level exceeds its yield stress [28, 40].

4. Strength Criterion for the SDM

Based on the homogenization theory of heterogeneous materials [43] and considering the breakage mechanics of geomaterials [44], Shen [45] proposed the binary medium model for structured soil and suggested a basic equation for the mean stress tensor $\{\overline{\sigma}\}$ as Equation (1). In the model, the

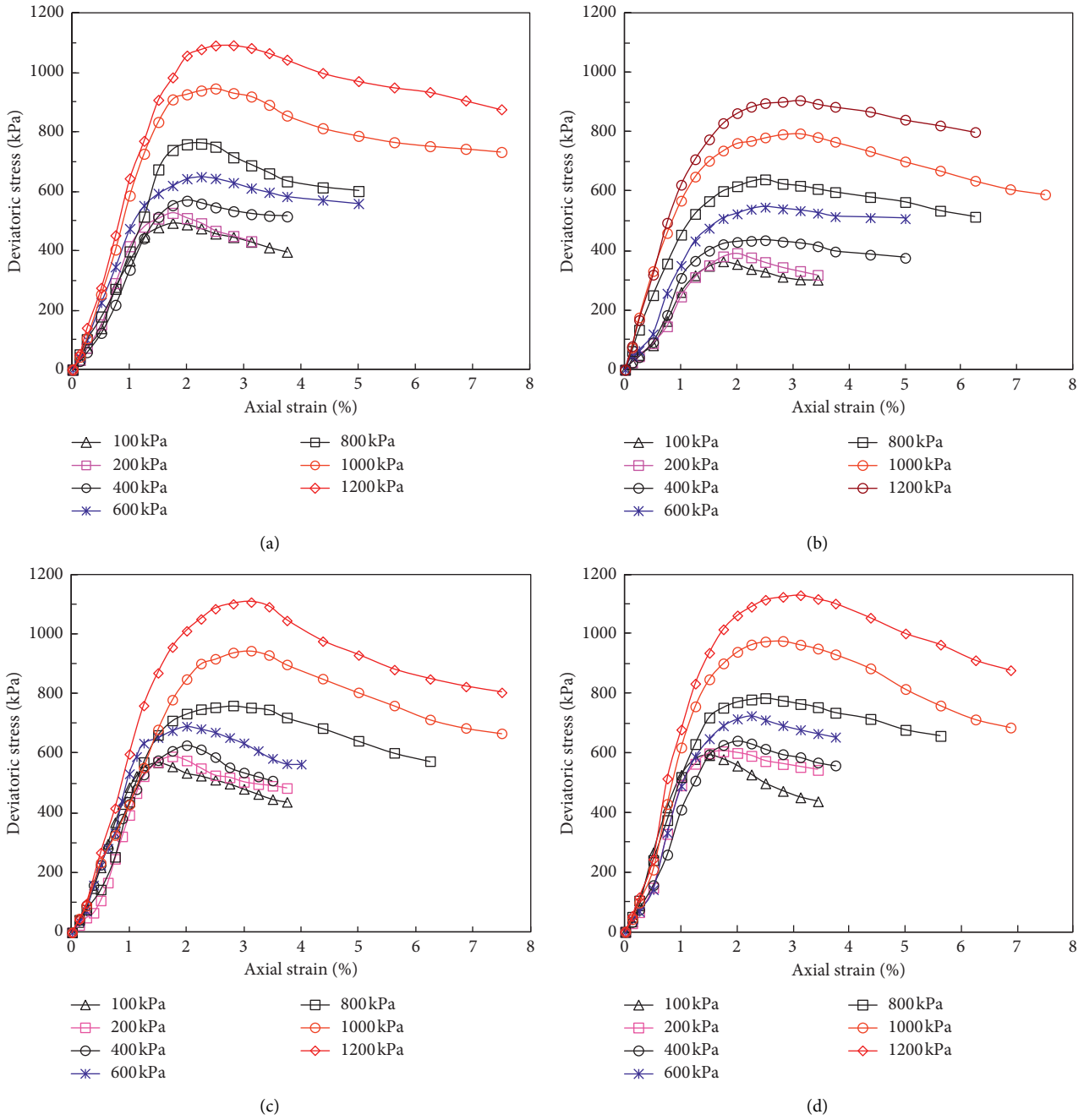

Figure 5: Relationship between deviatoric stress and axial strain at different applied confining pressures: (a) 2.5W+C100+P40, (b) 3.0W+C100+P70, (c) 3.0W+C200, and (d) 3.0W+C200+P50.

structured soil is conceptualized as binary medium consisting of bonding element and frictional element:

$$\{\overline{\sigma}\} = (1-b)\{\sigma_i\}b + \{\sigma_f\}, \tag{1}$$

where $\{\overline{\sigma}_i\}$ is the mean stress tensor of the bonding element and $\{\overline{\sigma}_f\}$ is the mean stress tensor of the frictional element, respectively, and b is the resistance share ratio.

In addition, according to the basic theory of soil mechanics, cohesion is independent of the normal stress, whereas internal friction is the proportional function of normal stress in the shear surface. Hence, the shear strength of the SDM can be expressed as

$$\tau = f(\tau_b) + f(\tau_f), \tag{2}$$

where $f(\tau_b)$ is the shear strength provided by the bonding element and $f(\tau_f)$ is the shear strength provided by the frictional element.

Substituting Equation (1) into (2), the shear strength of solidified soil can be expressed as

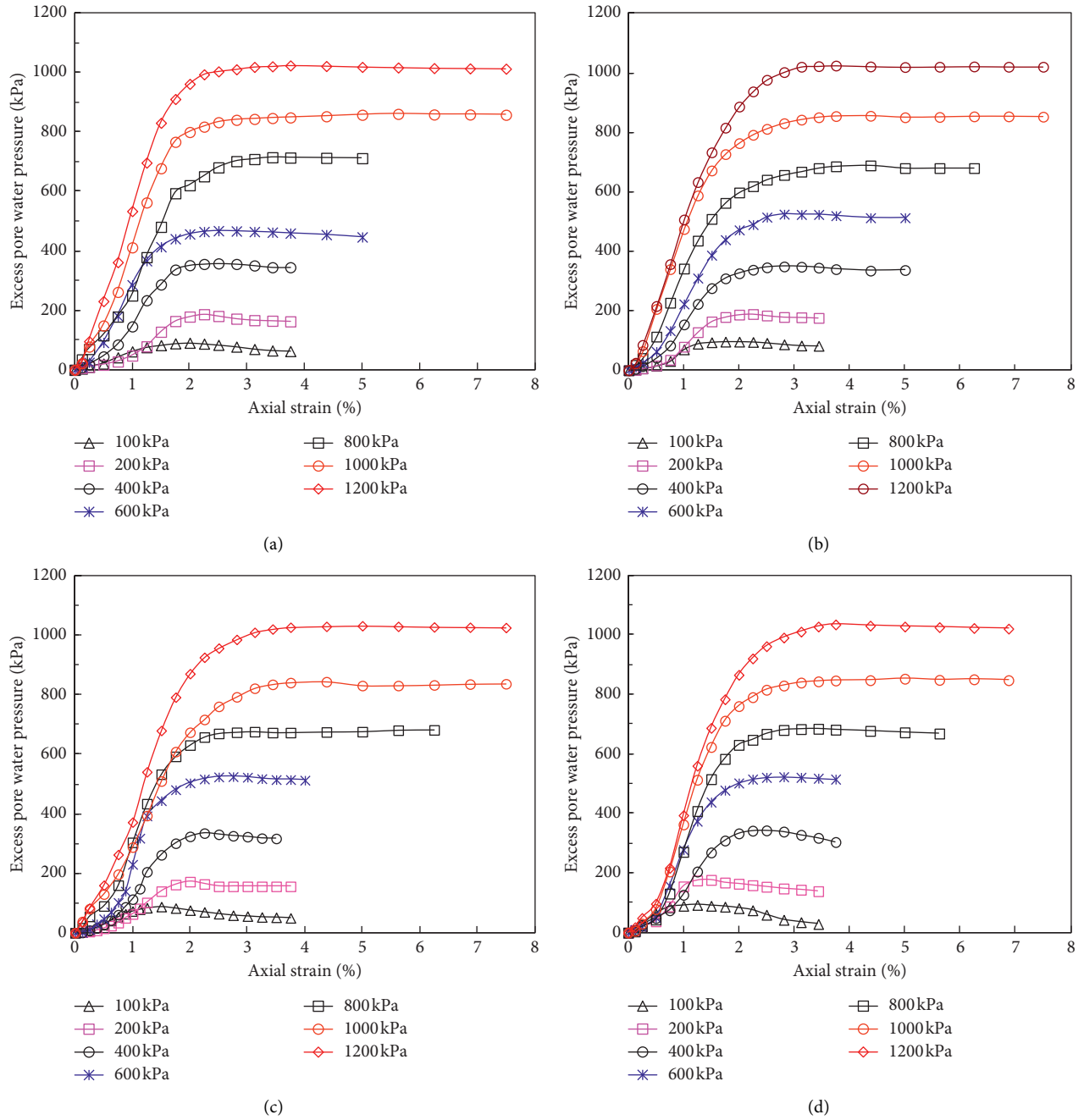

Figure 6: Relationship between excess pore water pressure and axial strain at different applied confining pressures: (a) 2.5W+C100+P40, (b) 3.0W+C100+P70, (c) 3.0W+C200, and (d) 3.0W+C200+P50.

$$\tau = (1-\beta)\tau_b + \beta\tau_f, \tag{3}$$

where τ_b and τ_f are the shear strengths provided by bonding element and frictional element, respectively, and β is the shear resistance share ratio.

It has been well documented that atmospheric pressure can be used in the strength reference framework to investigate the strength of the solidified soil [14, 46, 47]. The expression of shear strength provided by bonding element is assumed as follows:

$$\tau_b = \frac{q_u}{2}\left(\sigma_{bm}/P_a\right)^n, \tag{4}$$

where q_u is the unconfined compressive strength, $\sigma_{bm} = (\sigma_{1b} + \sigma_{2b} + \sigma_{3b})/3$ is the mean stress of bonding element, P_a is the standard atmospheric pressure, and n is a undetermined constant.

The shear strength provided by frictional element follows the Mohr–Coulomb criterion. It is the proportional function of normal stress and can be expressed as

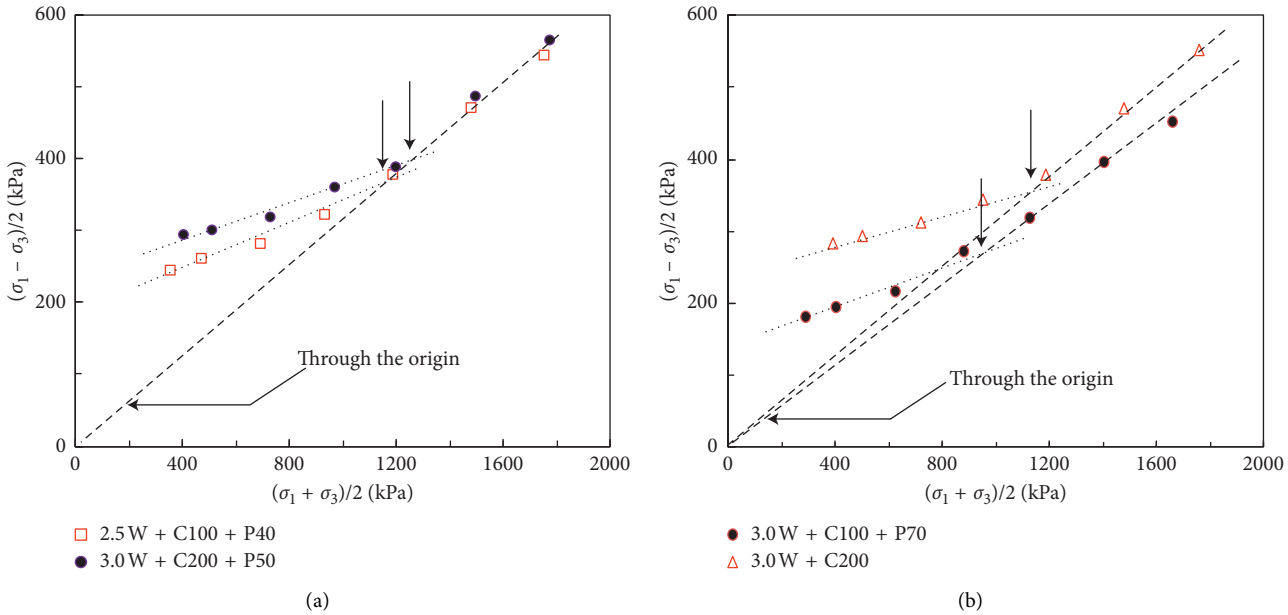

Figure 7: Undrained shear strength versus normal stress: (a) 2.5W+C100+P40 and 3.0W+C200+P50; (b) 3.0W+C100+P70 and 3.0W+C200.

$$\tau_f = \sigma_f \tan\varphi, \tag{5}$$

where φ is the internal friction angle of frictional elements and $\sigma_f = (\sigma_{1f} + \sigma_{3f})/3$ is the average of the minor principal stress and the major principal stress.

According to the triaxial tests data, the evolution law of shear strength is significantly different between the preyield state and the postyield state. The parameter β used here is introduced from the expression suggested by Liu and Shen [14], as shown in Equation (6):

$$\beta = 1 - e^{-(\sigma_3/\sigma_{vy})^m}, \tag{6}$$

where σ_{vy} is the structure yield stress which can be obtained from oedometer test and also can be indirectly derived from unconfined compression test according to the empirical relationship suggested by some researchers [27, 48, 49], σ_3 is the minor principal stress, and m is an undetermined constant.

Substituting Equations (4)–(6) into Equation (3), the shear strength criterion of the SDM can be expressed as follows:

$$\tau = e^{-(\sigma_3/\sigma_{vy})^m} \frac{q_u}{2} (\sigma_m/P_a)^n + \left[1 - e^{-(\sigma_3/\sigma_{vy})^m}\right] \sigma \tan\varphi, \tag{7}$$

where q_u is the unconfined compressive strength, $\sigma_m = (\sigma_1 + \sigma_2 + \sigma_3)/3$, and $\sigma = (\sigma_1 + \sigma_3)/2$.

5. Parameters Discussion and Strength Criterion Verification

5.1. Parameters Discussion. The influence of parameters m and n is discussed as follows. First, the influence of m is discussed with the assumption that n is a constant of 0.2 referenced the value suggested by Liu and Shen [14]. Other parameters are listed in Table 3. The influence of the parameter m to evolution laws of shear strength is shown in Figure 8. It can be seen that when $m = 0.1$, shear resistance is nearly one straight line and similar with the conventional Mohr–Coulomb criterion. In addition, it is interesting to note that when m is ≥3, not only all curves are very close but also the extensions of strength envelope are nearly through the origin in the postyield state. By comparison, the shape of curve is closer to the experimental curve when $m = 3$. Hence, $m = 3$ is suggested in this paper.

Table 3: Values of other parameters for "m" discussion.

P_a (kPa)	q_u (kPa)	σ_{vy} (kPa)	φ(°)
101.4	400	550	18

Subsequently, the value of n was discussed with the assumption that m is a constant of 3, and the other parameters are shown in Table 3. The influence of the parameter n to evolution laws of shear strength is shown in Figure 9. It can be seen that the parameter n has more significant influence when the stress level is lower; however, when the stress level is higher, the parameter n almost has no effect on shear resistance and all curves nearly concentrate to one straight line, what is more, with the extension of the strength envelope through the origin in the postyield state. Figure 9 indicates that the cohesion of bonding element gradually vanishes, and the shear resistance is mainly provided by the frictional element after structure yield. Hence, the proposed strength criterion can well describe the evolution laws of shear strength for the SDM.

5.2. Strength Criterion Verification. In order to further verify the validity of the proposed shear strength criterion,

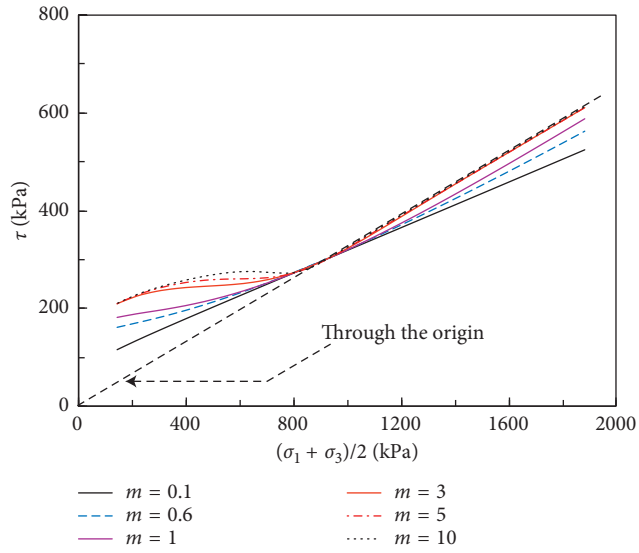

Figure 8: Influence of parameter m to evolution laws of shear strength.

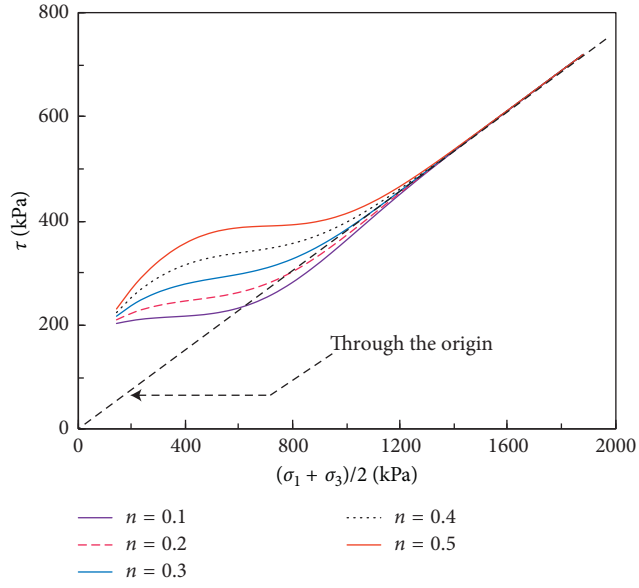

Figure 9: Influence of parameter (n) to evolution laws of shear strength.

comparisons between the simulation results obtained from the proposed strength criterion and the experimental data from triaxial tests are plotted in Figure 10. The parameters are determined as follows: $m = 3$, $P_a = 101.4$ kPa, σ_{vy} is determined according to one-dimensional compression test [27], q_u is determined according to unconfined compression test [50], φ is determined according to triaxial test in the postyield state, and n is an undetermined constant. The values of main parameters are summarized in Table 4.

Figure 10 presents comparisons of shear strength between simulation results and experimental data. The curve is mainly composed of two segments, the former is a slightly upward curve and the latter is nearly one straight line. The suggested range of n is 0.1–0.3. And it can be seen that the extension of strength envelope is nearly through the origin when stress level is higher. The comparisons between predicted results and experimental data demonstrate that the proposed strength criterion is valid, and it can well describe the mechanical features and shear strength evolution laws.

Figure 11 presents the evolution laws of percentage of cohesion and internal friction with the increase in the normal stress for the mixing proportion of 2.5W+C100+P40, and the others are same. It can be seen that the total shear resistance is all provided by the bonding element at first, and the percentage of cohesion decreases gradually with the increase in the stress level. However, the

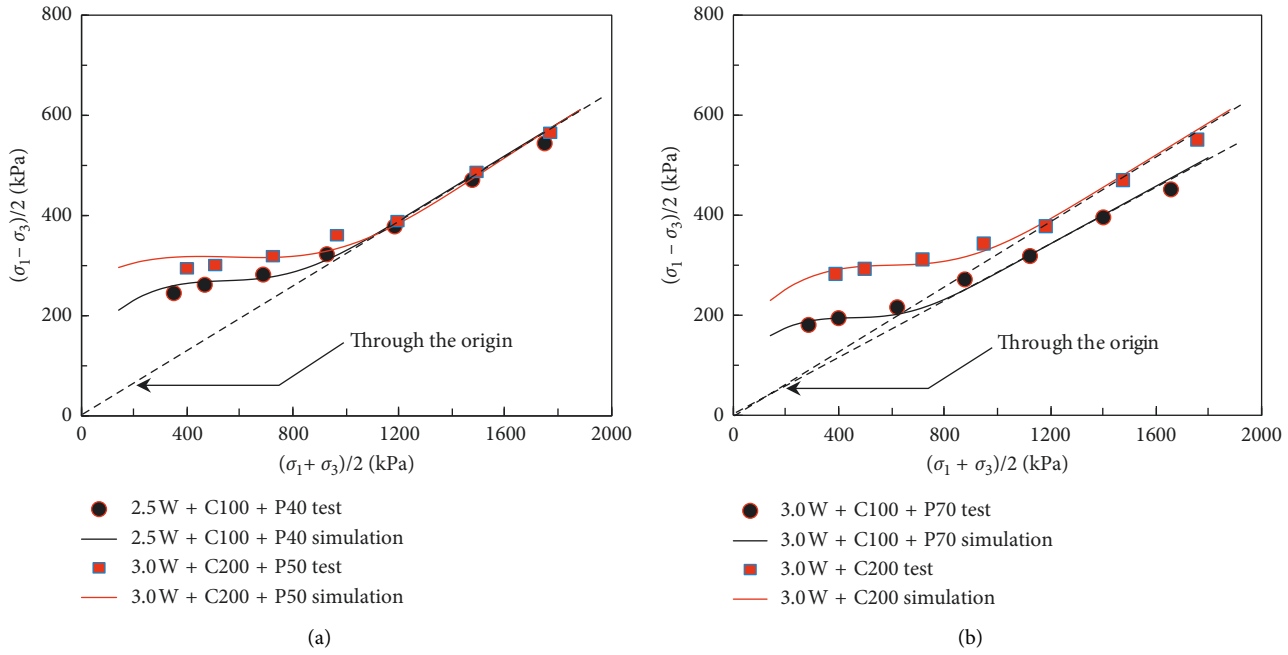

Figure 10: Comparisons between simulation results and test data: (a) 2.5W+C100+P40 and 3.0W+C200+P50; (b) 3.0W+C100+P70 and 3.0W+C200.

Table 4: Values of parameters for strength criterion verification.

Mixing proportion	Curing period	m	n	q_u (kPa)	σ_{vy} (kPa)	$\varphi(^\circ)$
2.5W+C100+P40	28	3	0.3	392	510	18
3.0W+C100+P70	28	3	0.3	305	436	16
3.0W+C200	28	3	0.3	426	559	18
3.0W+C200+P50	28	3	0.1	621	760	18

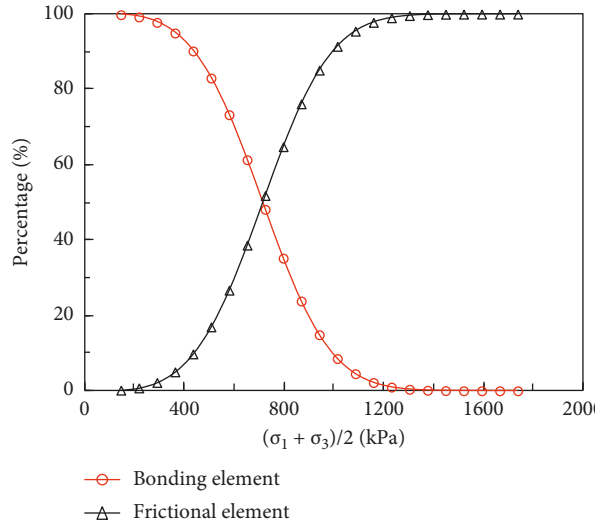

Figure 11: Percentage of cohesion and internal friction versus normal stress.

percentage of the internal friction increases with the increase in the stress level. Finally, with the bonding elements broken completely, the total shear resistance is fully provided by the frictional elements. Figure 11 indicates that the internal friction increases gradually with the increase in the stress level because of the bonding elements progressively breaking down and turning into frictional elements in essence.

6. Conclusions

The main conclusions obtained in this study are summarized as follows:

(1) The peak deviator stress increases small when the confining pressure is low, for the change of the fabric in the consolidation process is insignificant at low confining pressures.

(2) The undrained shear strength envelope is approximately consisted of two straight lines. The strength increases slightly with the increase in normal stress in preyield state; however, it increases significantly in postyield state with the extension of the strength envelope nearly through the origin.

(3) In preyield state, the shear strength of the SDM is mainly affected by cementation bonding effect and governed by structure resistance; however, in postyield state, it is mainly attributed to internal friction and controlled by the applied normal stress.

(4) A strength criterion considering strength evolution mechanism is proposed for the SDM. Comparisons of the predicted results and experimental data demonstrate that the proposed strength criterion can properly describe the mechanical features and strength evolution laws.

Data Availability

The data used to support the findings of this study are available from the corresponding author upon request.

Conflicts of Interest

The authors declare that they have no conflicts of interest.

Acknowledgments

This study was partially supported by the National Science and Technology Support Program Fund of China (Grant no. 2015BAB07B06), National Natural Science Foundation of China (Grant nos. 51378118 and 51608312), and Ministry of Water Resources Special Fund of China (Grant no. 201401006). The authors are grateful to Dr. Tao Cheng and Dr. Dong Tang for their constructive discussions, which are essential to the successful completion of this manuscript.

References

[1] C. I. Chiu, W. Zhu, and C. L. Zhang, "Yielding and shear behaviour of cement-treated dredged materials," *Engineering Geology*, vol. 103, no. 1, pp. 1–12, 2008.

[2] J. W. Ding, Z. S. Hong, and S. Y. Liu, "Triaxial shear test of flow-solidified soil of dredged clays," *Journal of Southeast University (Natural Science Edition)*, vol. 41, no. 5, pp. 1070–1074, 2011, in Chinese.

[3] V. Dubois, N. E. Abriak, R. Zentar, and G. Ballivy, "The use of marine sediments as a pavement base material," *Waste Management*, vol. 29, no. 2, pp. 774–782, 2009.

[4] Y. T. Kim, J. Ahn, W. J. Han, and M. A. Gabr, "Experimental evaluation of strength characteristics of stabilized dredged soil," *Journal of materials in civil engineering*, vol. 22, no. 5, pp. 539–544, 2009.

[5] Y. Tang, Y. Miyazaki, and T. Tsuchida, "Practices of reused dredgings by cement treatment," *Soils and Foundations*, vol. 41, no. 5, pp. 129–143, 2001.

[6] W. Zhu, C. L. Zhang, and A. C. Chiu, "Soil-water transfer mechanism for solidified dredged materials," *Journal of Geotechnical and Geoenvironmental Engineering*, vol. 133, no. 5, pp. 588–598, 2007.

[7] D. G. Grubb, M. Chrysochoou, C. J. Smith, and N. E. Malasavage, "Stabilized Dredged Material. I: Parametric Study," *Journal of Geotechnical and Geoenvironmental Engineering*, vol. 136, no. 8, pp. 1011–1024, 2010.

[8] K. Siham, B. Fabrice, A. N. Edine, and D. Patrick, "Marine dredged sediments as new materials resource for road construction," *Waste Management*, vol. 28, no. 5, pp. 919–928, 2008.

[9] L. L. Zeng, Z. S. Hong, and Y. J. Cui, "On the volumetric strain-time curve patterns of dredged clays during primary consolidation," *Géotechnique*, vol. 65, no. 12, pp. 1023–1028, 2015.

[10] M. Kamon, J. Jeoung, and T. Inui, "Alkalinity control properties of the solidified/stabilized sludge by a low alkalinity additive," *Soils and Foundations*, vol. 45, no. 1, pp. 87–98, 2005.

[11] J. K. Mitchell, "Practical problems from surprising soil behavior," *Journal of Geotechnical Engineering*, vol. 112, no. 3, pp. 259–289, 1986.

[12] J. B. Burland, "On the compressibility and shear strength of natural clays," *Géotechnique*, vol. 40, no. 3, pp. 329–378, 1990.

[13] F. Cotecchia and R. J. Chandler, "A general framework for the mechanical behaviour of clays," *Géotechnique*, vol. 50, no. 4, pp. 431–447, 2000.

[14] E. Liu and Z. Shen, "On the strength criterion for the structured soils," *Engineering Mechanics*, vol. 24, no. 2, pp. 50–55, 2007, in Chinese.

[15] Z. Hong, S. Shen, Y. Deng, and T. Negami, "Loss of soil structure for natural sedimentary clays," *Proceedings of the Institution of Civil Engineers-Geotechnical Engineering*, vol. 160, no. 3, pp. 153–159, 2007.

[16] H. Matsuoka and T. Nakai, "Stress-deformation and strength characteristics of soil under three different principal stresses," *Proceedings of the Japan Society of Civil Engineers*, vol. 232, pp. 59–70, 1974.

[17] Y. P. Yao, D. Lu, A. N. Zhou, and B. Zou, "Generalized nonlinear strength theory and transformed stress space," *Science in China Series E: Technological Sciences*, vol. 47, pp. 691–709, 2004.

[18] Y. P. Yao, J. Hu, A. N Zhou, T. Luo, and N. Wang, "Unified strength criterion for soils, gravels, rocks, and concretes," *Acta Geotechnica*, vol. 10, pp. 749–759, 2015.

[19] A. N. Zhou, R.-Q. Huang, and D. Sheng, "Capillary water retention curve and shear strength of unsaturated soils," *Canadian Geotechnical Journal*, vol. 53, pp. 974–987, 2016.

[20] H. Hanzawa and K. Adachi, "Overconsolidation of alluvial clays," *Soils and Foundations*, vol. 23, no. 4, pp. 106–118, 1983.

[21] S. Horpibulsuk, N. Miura, and D. T. Bergado, "Undrained shear behavior of cement admixed clay at high water content," *Journal of Geotechnical and Geoenvironmental Engineering*, vol. 130, no. 10, pp. 1096–1105, 2004.

[22] Y. Huang, W. Zhu, X. Qian, N. Zhang, and X. Zhou, "Change of mechanical behavior between solidified and remolded

solidified dredged materials," *Engineering Geology*, vol. 119, no. 3, pp. 112–119, 2011.

[23] D. W. Hight, R. Böese, A. P. Butcher, C. R. I. Clayton, and P. R. Smith, "Disturbance of the Bothkennar clay prior to laboratory testing," *Géotechnique*, vol. 42, no. 2, pp. 199–217, 1992.

[24] Z. Hong and T. Tsuchida, "On compression characteristics of Ariake clays," *Canadian Geotechnical Journal*, vol. 36, no. 5, pp. 807–814, 1999.

[25] S. Leroueil and P. Vaughan, "The general and congruent effects of structure in natural soils and weak rocks," *Géotechnique*, vol. 40, no. 3, pp. 467–488, 1990.

[26] J. H. Schmertmann, "The mechanical aging of soils," *Journal of Geotechnical Engineering*, vol. 117, no. 9, pp. 1288–1330, 1991.

[27] J. W. Ding, X. C. Wu, H. Li, X. Bie, and F. Ji, "Compression properties and structure yield stress for solidified soil of dredged clays," *Journal of Engineering Geology*, vol. 20, no. 4, pp. 627–632, 2012, in Chinese.

[28] A. H. M. Kamruzzaman, S. H. Chew, and F. H. Lee, "Structuration and destructuration behaviour of cement-treated Singapore marine clay," *Journal of Geotechnical and Geoenvironmental Engineering*, vol. 135, no. 4, pp. 573–589, 2009.

[29] S. H. Chew, A. H. M. Kamruzzaman, and F. H. Lee, "Physicochemical and engineering behaviour of cement treated clays," *Journal of Geotechnical and Geoenvironmental Engineering*, vol. 130, no. 7, pp. 696–706, 2004.

[30] Z. S. Hong, J. Yin, and Y. J. Cui, "Compression behaviour of reconstituted soils at high initial water contents," *Géotechnique*, vol. 60, no. 9, pp. 691–700, 2010.

[31] A. B. Parreira, A. R. K. Kobayashi, and O. B. Silvestre Jr., "Influence of Portland cement type on unconfined compressive strength and linear expansion of cement-stabilized phosphogypsum," *Journal of Geoenvironmental Engineering*, vol. 129, no. 10, pp. 956–960, 2003.

[32] W. Shen, M. Zhou, and Q. Zhao, "Study on lime–fly ash–phosphogypsum binder," *Construction and Building Materials*, vol. 21, no. 7, pp. 1480–1485, 2007.

[33] H. Tayibi, M. Choura, F. A. López, F. J. Alguacil, and A. López-Delgado, "Environmental impact and management of phosphogypsum," *Journal of Geoenvironmental Engineering*, vol. 90, no. 8, pp. 2377–2386, 2009.

[34] G. Xu, F. Gao, Z. Hong, and J. Ding, "Sedimentation behavior of four dredged slurries in China," *Marine Georesources and Geotechnology*, vol. 30, no. 2, pp. 143–156, 2012.

[35] T. Luo, Y. P. Yao, A. N. Zhou, and X. G. Tian, "A three-dimensional criterion for asymptotic states," *Computers and Geotechnics*, vol. 41, pp. 90–94, 2012.

[36] J. K. Mitchell, *Fundamentals of Soil Behavior*, Wiley, New York, NY, USA, 2nd edition, 1992.

[37] Y. P. Yao, W. Hou, and A. N. Zhou, "Constitutive model for overconsolidated clays," *Science in China Series E: Technological Sciences*, vol. 51, pp. 179–191, 2008.

[38] Y. P. Yao, W. Hou, and A. N. Zhou, "UH model: three-dimensional unified hardening model for overconsolidated clays," *Géotechnique*, vol. 59, pp. 451–469, 2009.

[39] Y. P. Yao and A. N. Zhou, "Non-isothermal unified hardening model: a thermo-elastoplastic model for clays," *Géotechnique*, vol. 63, pp. 1328–1345, 2013.

[40] S. M. Rao and P. Shivananda, "Compressibility behaviour of lime-stabilized clay," *Geotechnical and Geological Engineering*, vol. 23, no. 3, pp. 309–319, 2005.

[41] F. Sariosseiri and B. Muhunthan, "Effect of cement treatment on geotechnical properties of some Washington state soils," *Engineering Geology*, vol. 104, no. 1, pp. 119–125, 2009.

[42] J. Suebsuk, S. Horpibulsuk, and M. D. Liu, "Modified structured cam clay: a generalised critical state model for destructured, naturally structured and artificially structured clays," *Computers and Geotechnics*, vol. 37, no. 7, pp. 956–968, 2010.

[43] J. Wang, C. Leung, and Y. Ichikawa, "A simplified homogenisation method for composite soils," *Computers and Geotechnics*, vol. 29, no. 6, pp. 477–500, 2002.

[44] Y. G. Chen, L. Y. Jia, W. M. Ye, B Chen, and Y. J. Cui, "Advances on experimental investigation on hydraulic fracturing behavior of bentonite-based materials used for HLW disposal," *Environmental Earth Sciences*, vol. 75, pp. 787–800, 2016.

[45] Z. Shen, "Breakage mechanics for geological materials: An ideal brittle-elastic-plastic model," *Chinese Journal of Geotechnical Engineering*, vol. 25, no. 3, pp. 253–257, 2003, in Chinese.

[46] G. A. Lorenzo and D. T. Bergado, "Fundamental parameters of cement-admixed clay-new approach," *Journal of Geotechnical and Geoenvironmental Engineering*, vol. 130, no. 10, pp. 1042–1050, 2004.

[47] P. Jongpradist, S. Youwai, and C. Jaturapitakkul, "Effective void ratio for assessing the mechanical properties of cement-clay admixtures at high water content," *Journal of Geotechnical and Geoenvironmental Engineering*, vol. 137, no. 6, pp. 621–627, 2011.

[48] S. Horpibulsuk, D. T. Bergado, and G. A. Lorenzo, "Compressibility of cement-admixed clays at high water content," *Géotechnique*, vol. 54, no. 2, pp. 151–154, 2004.

[49] Y. Tang, H. Liu, and W. Zhu, "Study on engineering properties of cement-stabilized soil," *Chinese Journal of Geotechnical Engineering*, vol. 22, no. 5, pp. 549–554, 2000, in Chinese.

[50] J. W. Ding, T. P. Liu, Y. P. Cao, R. M. Yang, and G. Wang, "Unconfined compression tests and strength prediction method for solidified soils of dredged clays with high water content," *Chinese Journal of Geotechnical Engineering*, vol. 35, no. 2, pp. 55–60, 2013, in Chinese.